Proceedings World Geothermal Congress 2020+1
Reykjavik, Iceland, April - October 2021

Design and Operation of Testing Facility for Investigation of Novel Corrosion Resistant Coatings for High Temperature Geothermal Applications

Danyil Kovalov[a,c], Jan Přikryl[a,b], Gifty Oppong Boakye[a], Andri Ísak Thorhallson[a], Ioana Csaki[d], Sigrún Nanna Karlsdóttir[a,b]

[a]Department of Industrial Engineering, Mechanical Engineering and Computer Science, University of Iceland, Reykjavik, Iceland

[b]Gerosion Ltd., Árleynir 2-8, IS-112 Reykjavik, Iceland

[c]Volodymyr Dahl East Ukrainian National University, Severodonetsk, 93400, Ukraine

[d]Department of Engineering and Management of Metallic Materials Production Polytechnic, University of Bucharest, Romania

dankov@hi.is, janp@hi.is, gob13@hi.is, ath196@hi.is, ioana.apostolescu@upb.ro, snk@hi.is

Keywords: CO_2/H_2S Corrosion; High Temperature Corrosion; Geothermal Environment; Geo-Coat.

ABSTRACT

The rapid corrosive damage of the equipment operating in the aggressive geothermal environment requires the development of novel cost-effective corrosion resistant coatings with design to increase the materials' service life. In this work, a developed laboratory facility for simulating a two-phase geothermal environment (i.e., gas/liquid) to investigate the corrosion resistant coatings for high temperature geothermal applications is presented. Using the developed facility, the simulated geothermal environment with a pH of 4 at T=185 °C and P=7 bar, consisting of a gas phase (i.e., vapor) and H_2S and CO_2 gases, was established as experimental conditions. For the trial high temperature corrosion testing, high entropy alloy (HEA) coatings of CoCrFeNiMo and $Al_{0.5}$CrFeNiCo were developed. The duration of the trial high temperature corrosion tests in a flow-through reactor was 96 hours. After testing, using EDS analysis, deposited sulfur was found in both the tested coatings. Using the microstructure SEM analysis, localized corrosion in the tested CoCrFeNiMo coating was detected, whereas the surface of $Al_{0.5}$CrFeNiCo coating was more corrosion resistant to simulated geothermal environment.

1. INTRODUCTION

The corrosive nature of the geothermal environment, including effects of high temperature and fluid chemical composition on the metallic parts, leads to corrosion damage of the geothermal plant facilities, and hence, to decreasing their service life (Karlsdottir, 2012). This can result in premature material failure and cause disruption of geothermal energy production in geothermal power plants. The main corrosive species which are present in the geothermal fluid (steam/water) include non-condensable gases (NCG) containing carbon dioxide (CO_2), hydrogen sulfide (H_2S), as well as aggressive [Cl^-] and [SO_4^{2-}] ions (Stefánsson, 2017). As known, the extracted geothermal fluid travels through the power plant system (i.e., pipeline, rotor blades, stator blades, rotor, labyrinth seals, etc.); therefore, the fluid and gas composition vary according to changes in the system conditions. For example, within the Hellisheiði geothermal power plant in Iceland studied within the GeoCoat project, the conditions in different locations where fluid was sampled showed different environmental conditions, including temperature, pressure and chemical content (Sigurðardóttir et al., 2018). The chemical content of the geothermal fluid for each point is presented in Table 1. It is seen that at the geothermal plant, the listed environmental conditions have a wide range of temperature, pressure, pH, as well as CO_2/H_2S gas and Cl^- and SO_4^{2-} ion concentrations, effect of which can subsequently lead to nucleation of different corrosion damage of the materials used. In Ref. (Karlsdottir, 2012) is shown that using a widely applied alloy (e.g., carbon steel) in a liquid medium with a pH lower than 9.5 results in the faster dissolution process with the occurrence of uniform corrosion on the alloy surface due to the inability to passivation, whereas, in pH ranging from 9.5 to 14, carbon steel obtains the ability to spontaneous passivation with decreasing the corrosion rate (Kovalov et al., 2019).

Nevertheless, carbon steel exposed to geothermal steam (i.e., gas phase) can form a partially protective pyrite film on the surface, even at a pH being lower than 9.5 (down to pH=6), leading to the lower dissolution process of the carbon steel. Increasing the liquid temperature can change the environmental effect on alloys since the increased temperature leads to increasing the rates of the chemical/electrochemical reactions in the system, resulting in higher corrosion rates (Kovalov et al., 2019). As described above, the geothermal environment contains volcanic gases, namely CO_2 and H_2S, that are aggressive from their nature. Furthermore, anions of Cl^-, S^{-2}, SH^- are also part of the geothermal environment where Cl^- ions exist as products of ocean water (or volatile chloride from HCl gas) and S^{-2}, SH^- ions are from the volcanic gas system (Karlsdottir and Jonsson, 2018). These listed ions of the gases also promote corrosion of alloys. Therefore, the increased temperature, different pH, and various aggressive species content in the geothermal environment lead to instability of the fluid system with resulting in the aggressive ions may be transported across the medium to the metal surface and break the passive layer (in the case of passivated alloys) with subsequent penetration into the metal, and hence, the localized corrosion nucleates that can lead to higher corrosion rates. The high corrosion rates in metals may be reduced using high-grade alloys, for example, Inconel 600 or Hastelloy C-276; however, due to their costliness, such alloys are not economically viable for a total replacement of already existing parts of geothermal power plants.

Therefore, the Geo-Coat project is called to develop novel and cost-effective corrosion resistant coatings for widely used steel alloys, which will be able to effectively to operate in high-temperature geothermal conditions with the subsequent decrease in losses from corrosion.

Table 1: The range of the properties and chemical composition at the different sampling location at Hellisheidi and Nesjavellir, Iceland (Sigurðardóttir et al., 2018).

no.	Location	State	T [°C]	P [bar]	pH	CO_2 [mg/kg]	H_2S [mg/kg]	SiO_2 [mg/kg]	Na [mg/kg]	Ca [mg/kg]	Cl [mg/kg]	SO_4 [mg/kg]	Se [mg/kg]
1	Wellhead	Water	176 - 209	16 - 17	7.16 - 8.67	4 - 29.1	7 - 105	204 - 1224	9.5 - 168.7	< 0.32 - 0.46	5 - 205	1.5 - 13.4	0.82 - 46.9
		Cond. Steam	-	-	3.95 - 4.42	-	-	0.172 - 0.53	< 0.1 - 0.13	< 0.1	0.08 - 1.8	0.3 - 1.6	< 0.5 - 1.43
		NCG	-	-	-	443 - 68	410 - 1173	-	-	-	-	-	-
2	Steam into turbines	NCG	172 - 191	7.4 - 11.8	-	1268 - 3470	384 - 978	-	-	-	-	-	-
3	Separator water after 1st flash	Water	172 - 180	8.4 - 12	8.70 - 8.94	22 - 30	50 - 75	676 - 758	168 - 206	0.30 - 0.74	155 - 186	42705	n.a.
4	Separator water after 2nd flash	Water	119	2 - 10	9.2	20	30	735	203	0.85	186	21.5	16
5	Separator water after heat exchangers	Water	10 - 85	10 - 12	8.83 - 9.2	19.8 - 23.7	30 - 82	735 - 764	159 - 206	0.27 - 0.78	118 - 186	18.1 - 24.4	7.6 - 15.3
6	Condensate from condenser outlet	Water	40 - 60	1	5.1 - 6.9	2 - 20.9	1 - 98.3	< 0.06 - 4.4	< 0.1 - 1.78	< 0.1 - 0.86	< 0.1 - 1	1 - 3.9	< 0.5
7	Cooling water	Water	4	n.a.	7.3	25.7	0	24	6.3	4.56	5.8	1.4	< 0.5
8	Typical ground-water	Water	-	-	7.72 - 8.3	-	-	24.1 - 34.9	6.2 - 14.8	4.8 - 9.5	7.0 - 13.2	2.2 - 10.5	< 0.5

In this paper, we present a developed laboratory test facility for the investigation of novel corrosion resistant coatings for high temperature geothermal applications. For running a trial test in the simulated geothermal environment in the laboratory, the two High Entropy Alloy coatings of CoCrFeNiMo and $Al_{0.5}CrFeNiCo$ for a stainless steel substrate of AISI 304 were developed.

The geothermal environment can be established by mimicking natural geothermal conditions in the laboratory flow-through reactor shown in Figure 1. Using this experimental system depicted in Figure 1, it is possible to replicate geothermal fluid with physical and geochemical properties including temperature, pressure and geochemical composition and the mass flow, particularly one-phase (i.e., liquid) or two-phase (i.e., liquid-gas) flow. The advantage of such an experimental approach is the controlled selection of testing parameters. The goal is to achieve the desired simulated geothermal environment for testing the corrosion resistance of novel Geo-Coat coatings intended to be used for protecting substrate alloys used in geothermal power production. The corrosion testing is performed using a system with a continuous flow of simulated geothermal fluid interacting with the specimens in the flow-through reactors (FTR). In this way, the different parameters and chemistry allow for the comprehensive testing outcome, with low to elevated temperature, pressure and CO_2 and H_2S concentrations, accounting variable conditions inside geothermal power plant systems can be simulated. Such variations can reveal different corrosion mechanisms and weak points of tested materials. The corrosion testing in the FTR includes low-pressure environment around vapor-water saturation curve and low to moderate H_2S and CO_2 concentrations ($\leq$350 ppm and $\leq$1000 ppm, respectively). The conditions selected for tests cover the conditions occurring within the power plant areas with significantly high corrosion potential, e.g., acidic pH and considerable H_2S and CO_2 content. Moreover, elevated Cl^- levels are typical for geothermal power plants located at sea-sides or relevant proximity. Using the simulated geothermal environment, the developed Geo-Coat coatings will be investigated for resistance to nucleation of localized corrosion such as pitting corrosion and initiation of cracks caused by stress corrosion cracking (SCC) that are known to occur in geothermal power plant components.

Figure 1: Laboratory facility with the flow-through reactor pipe. University of Iceland.

2. EXPERIMENTAL

2.1 Experimental setup

The experimental setup for high temperature corrosion experiments for investigation of coatings for geothermal applications in the Corrosion and Materials Laboratory at University of Iceland is depicted in Figure 2 and Figure 3. All wetted parts of the experimental apparatus were made of corrosion resistant alloys, including titanium, Hastelloy-C276, and Inconel 600 as well as of an inert material, including PEEK. The solutions were CO_2/H_2S gases are generated to simulate geothermal fluid is mixed with HCl solution and pumped into the 130 cm long working pipe reactor (i.e., the flow-through reactor pipe [FTRP]) with 3.34 cm inner diameter at a flow rate of 0.15 mL/min (for each solution), using High Performance Liquid Chromatography (HPLC) pumps (Chromtech®). The pressure is controlled at the end of the system line with aid of back pressure regulator, BPR. The FTRP is heated to the target temperature of 185 °C with the aid of a heating tubular oven (Carbolite) using a 3-zone independent temperature controlling system. The pressure is monitored with pressure gauge, PG, inside the line after the solution passes the heated FTRP section (Figure 2). The outlet fluid is cooled to room temperature with the help of a cooling loop placed between the FTRP and the back-pressure regulator. The outlet solution is collected at the low-pressure end of the back-pressure regulator. The inlet solutions are collected directly from the inlet solution tanks.

2.2 Geothermal fluid preparation

For tuning and designing the simulated geothermal environment for corrosion testing of coatings in the FTR, a software for geochemical calculations called PHREEQC is used with program version 3.4.0-12927, (Parkhurst and Appelo, 2013). The solutions are evaluated and calculated first based on the conditions listed in Table 1. The concept is based on the following: two solutions, one containing CO_2 and H_2S and another containing HCl, are prepared and stored separately to maintain their stability. Further, inlet solution #1 being a combination of Na_2S (0.010 mol/kg) + $NaHCO_3$ (0.046 mol/kg) is mix with inlet solution #2 (HCl 0.066 mol/kg) and pumped, with 1:1 ratio, into the reactor (see Figure 2). Corrosive CO_2/H_2S rich geothermal environment can thus be produced and maintained with a continuous flow of the simulated fluid. The mixed geothermal fluid that is heated up to 185 °C has concentrations of 0.033 mol/kg HCl, 0.005 mol/kg Na_2S, 0.023 mol/kg of $NaHCO_3$. The measured pH of mixed solutions was $\sim$4. The solution concentrations considered are selected not to exceed 350 ppm (10.3 mmol/kg) of H_2S, at any stage, to maintain relatively safe and non-life threating working environment in case of an accident (solution spill, etc.) for the staff operating the experimental setups (World Health Organization, 2003). Gas concentration (in case of gas leakage) is monitored with CO_2/H_2S gas sensors inside well-ventilated laboratory as well.

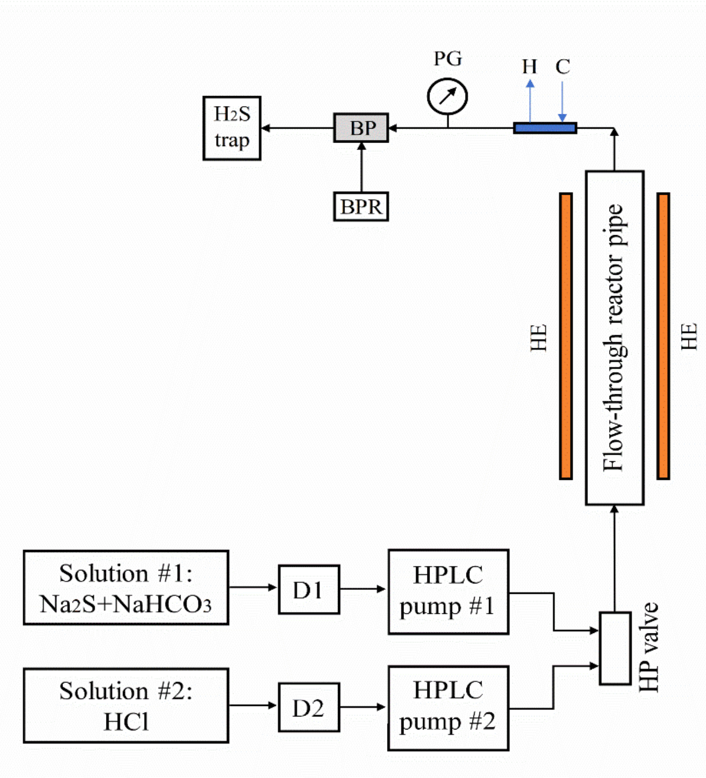

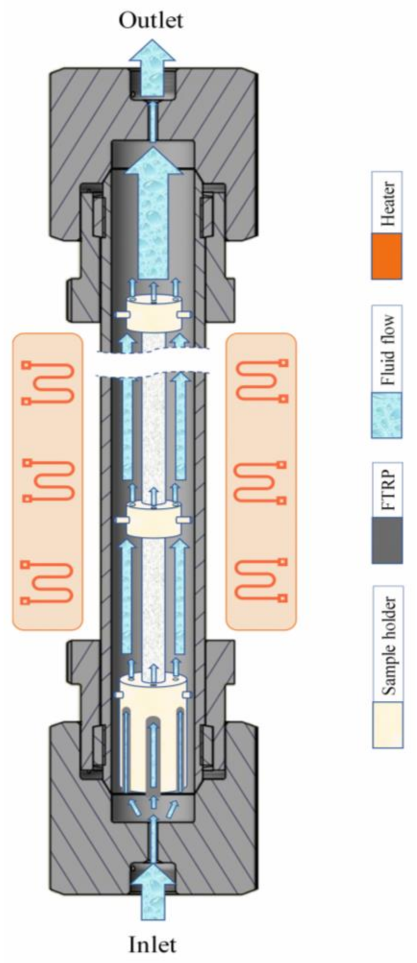

Figure 2: Scheme of the low pressure experimental setup: D1 – HPLC solvent degasser for solution #1; D2 – HPLC solvent degasser for solution #2; HP valve – high pressure valve; HE – heating element of the tubular oven (Carbolite); C – cold water in; H – hot water out; PG - pressure gauge; BP – booster pump; BPR – back-pressure regulator.

Figure 3: Illustration of the flow-through reactor pipe with sample holder inside.

Table 2: Calculated conditions and the fluid characteristics for the simulated geothermal environment in the FTRP.

pH	T [°C]	P [bar]	CO_2 [ppm]	H_2S [ppm]	Cl [ppm]	Na [ppm]	Phase condition
~4	185	7	1012	170	1202	759	Gas (vapor)

Two solutions are mixed in line prior to entering the FTRP; one solution consists of an H_2S/CO_2 rich solution made from Na_2S and $NaHCO_3$ (Sigma-Aldrich®) with a pH of ~9.5, whereas the other solution is an HCl solution (Sigma-Aldrich®) of a pH of ~1.3, also prepared with degassed deionized water. A fresh solution is made every three days to avoid oxidation of H_2S. For all experiments, the inlet solution was undersaturated with respect to sulfide and carbonate minerals. The CO_2 samples are collected to NaOH to prevent degassing. The analytical precision at the 95% confidence level based on repeated analysis of an internal standard is ~1–10% for different elements. Based on the duplicated determination, the analytical precision of CO_2 and H_2S concentrations is < 3%, and pH is ± 0.05 pH units. It is to be noted that the condition of the simulated geothermal fluid with parameters of T=185 C and P=7 bar is in the gas phase (i.e., vapor) with close to the two-phase condition of the fluid (i.e., gas/liquid).

2.3 Materials and analysis

High Entropy Alloys (HEA) of CoCrFeNiMo (Karlsdottir et al., 2019) and $Al_{0.5}$CrFeNiCo were chosen as materials for coating stainless steel substrates of AISI 304. The HEA coatings were realized by electrospark deposition technique and provided by a Geo-Coat partner from Politehnica University of Bucharest. The nominal composition of the HEA coatings is shown in Table 3. The fabricated coated samples were flat with dimensions of 8mm-width x 50mm-length x 4mm-height.

Table 3: Nominal composition for CoCrFeNiMo and $Al_{0.5}$CrFeNiCo.

Coating	Elements [at%]				
CoCrFeNiMo	Co = 20	Cr = 20	Fe = 20	Ni = 20	Mo = 20
$Al_{0.5}$CrFeNiCo	Al = 10	Cr = 22.5	Fe = 22.5	Ni = 22.5	Co = 22.5

Since the simulated geothermal environment might take a two-phase condition, including gas and/or liquid phases and taking into account that the liquid phase might be a cause of galvanic corrosion between the coated/bulk sample and a metallic sample holder, non-metallic Polyether Ether Ketone (PEEK) TECAPEEK® material was used for sample holder production. The PEEK sample holder well-resisted to acidic medium, high pressure, and temperature up to 300 °C, which complied with the experimental requirements. The dimensions of the PEEK sample holder of 15mm-diameter x 28mm-length are depicted in Figure 4. It is noted here that the presented sample holder can be used for both cylindrical and rectangular samples.

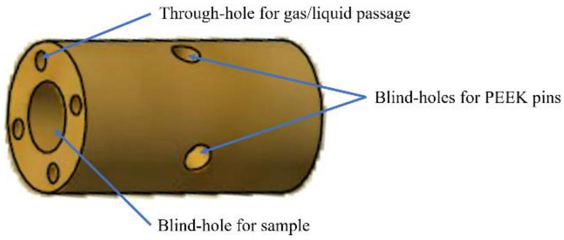

Figure 4: The sample holder used for the HEA specimens.

The demonstration of the PEEK sample holder tree with samples is shown in Figure 5. Using the sample holders, it is possible to hold both flat samples and rod samples. Since the inlet part of FTRP is located out of the heater, a PEEK sample holder stand was produced to increase the distance from the "cold zone" located on the FTRP bottom.

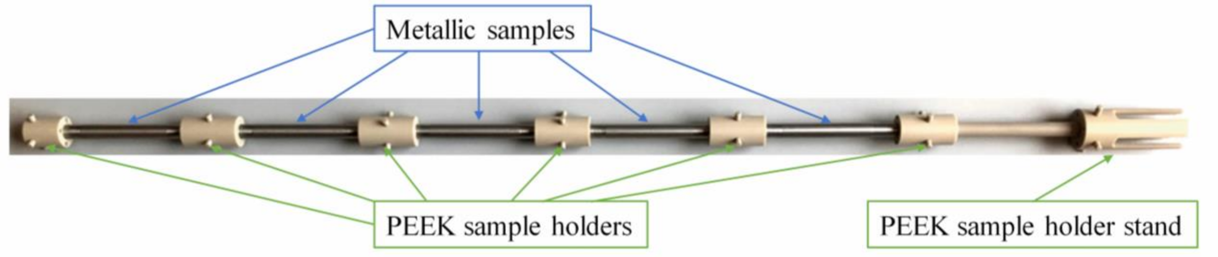

Figure 5: The PEEK sample holders assembled with rod samples for demonstration purpose.

The layout of the sample holders inside the FTRP is shown above in Figure 2. The microstructure and chemical composition of the tested HEA coatings were studied using SEM/EDS analysis.

3. RESULTS AND DISCUSSION

3.1 Microstructural and chemical composition analysis of CoCrFeNiMo and Al$_{0.5}$CrFeNiCo coatings

Figure 6 shows the SEM microstructure of CoCrFeNiMo coatings for non-tested (Figure 6a) and tested samples in the simulated geothermal solution of $N_2S+NaHCO_3+HCl$ with pH of 4 at T=185 ºC and P=7 bar (Figure 6b). From Figure 7, it was found that the tested and non-tested CoCrFeNiMo coatings have a porous surface where the tested sample reacted with the prepared solution with being precipitation found near the pits on the coating surface. Using EDS, chemical composition for corrosion tested CoCrFeNiMo coating was obtained where the components of the coating have a non-homogeneous distribution with sulfur (S) as well as oxygen (O) and carbon (C), deposited from the reaction of the coating to H_2S and CO_2 gases present in the environment. The distribution of the HEA components for CoCrFeNiMo surface after the experiment is shown in the table of Figure 7.

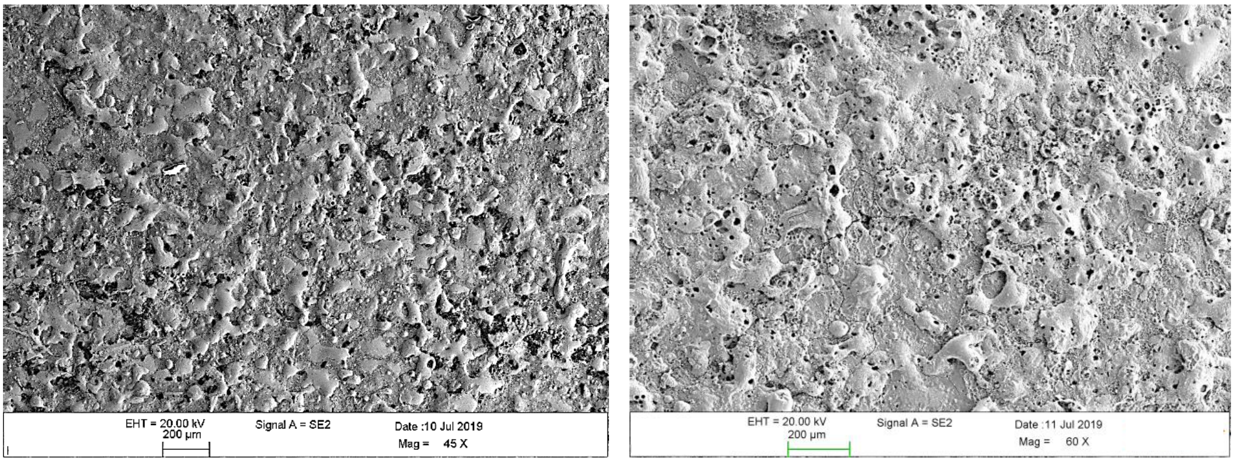

(a) (b)

Figure 6: SEM microstructure of CoCrFeNiMo coatings: (a) – non-tested; (b) – corrosion tested.

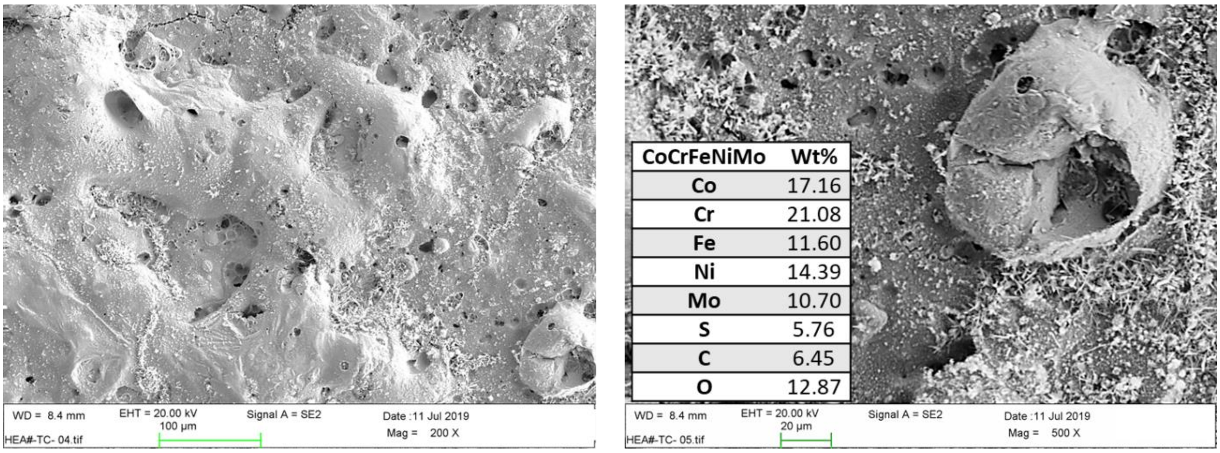

CoCrFeNiMo	Wt%
Co	17.16
Cr	21.08
Fe	11.60
Ni	14.39
Mo	10.70
S	5.76
C	6.45
O	12.87

(a) (b)

Figure 7: SEM microstructure of CoCrFeNiMo coating tested in the simulated geothermal solution with a pH of 4 at T=185 C and P=7 bar: (a) – lower magnification; (b) – higher magnification.

The existed pits in the coating surface contacting with the geothermal environment may transform to localized corrosion damage in the external surface with developing pitting corrosion. This is because the achieved gas phase in FTR is close to the point of water-saturation pressure, including two-phase flow (i.e., the gas/liquid phase). Therefore, an electrochemical effect of the liquid phase may occur, leading to the electrochemical potential drop from the external surface down to the pit bottom. This will result in the establishment of the anodic region on the pit bottom and cathodic region on the external surface that contributes to pit growth (Kovalov et al., 2019).

However, EDS mapping (Figure 8) for the cross-sectioned CoCrFeNiMo sample tested under given simulated geothermal conditions has shown the absence of sulfide corrosion product penetrated into the coating. In contrast, in the tested CoCrFeNiMo coating, the cracking was found that may be formed resulting from the residual stress due to thermal exposure during coating application.

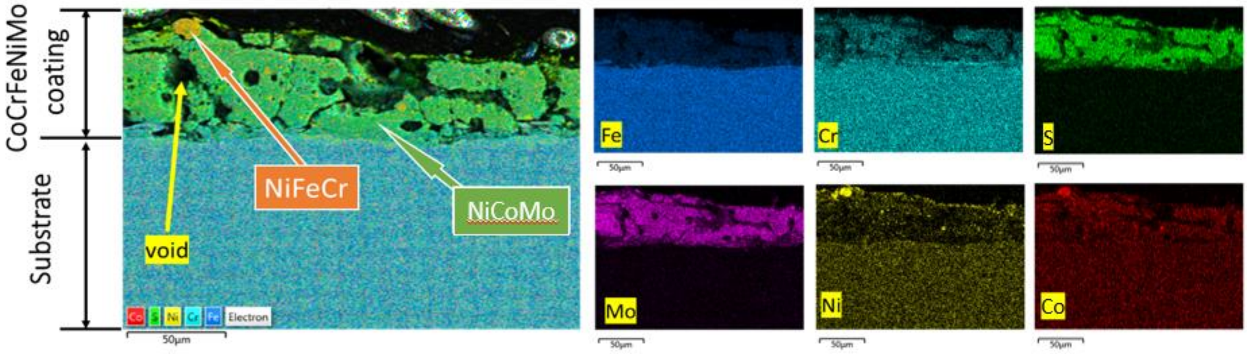

Figure 8: EDS mapping of CoCrFeNiMo coating tested in the simulated geothermal solution with a pH of 4 at T=185 C and P=7 bar.

The SEM analysis of the microstructure for $Al_{0.5}CrFeNiCo$ coating after tested in the simulated geothermal solution with pH of 4 at T=185 ºC and P=7 bar showed more promising results without visible local corrosion damage (see Figure 9b and Figure 10).

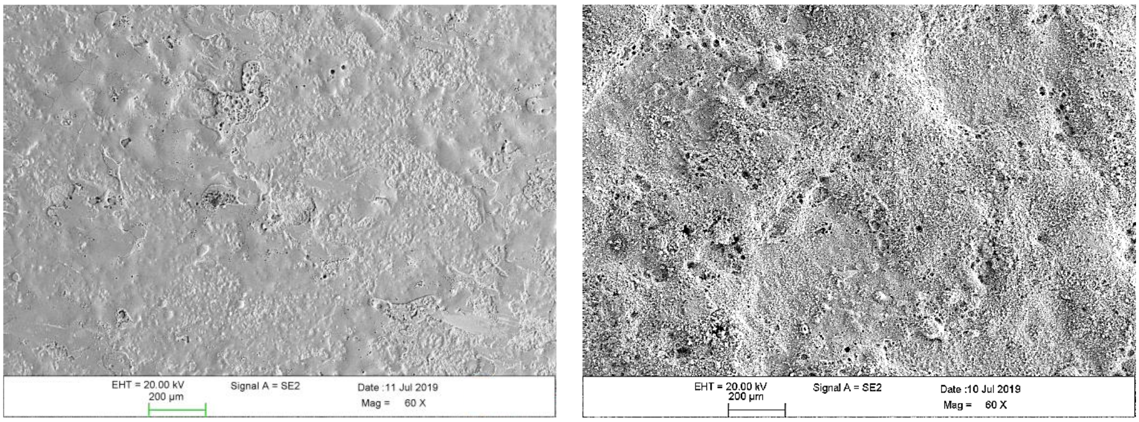

(a) (b)

Figure 9: SEM microstructure of $Al_{0.5}CrFeNiCo$ coatings: (a) – non-tested; (b) – corrosion tested.

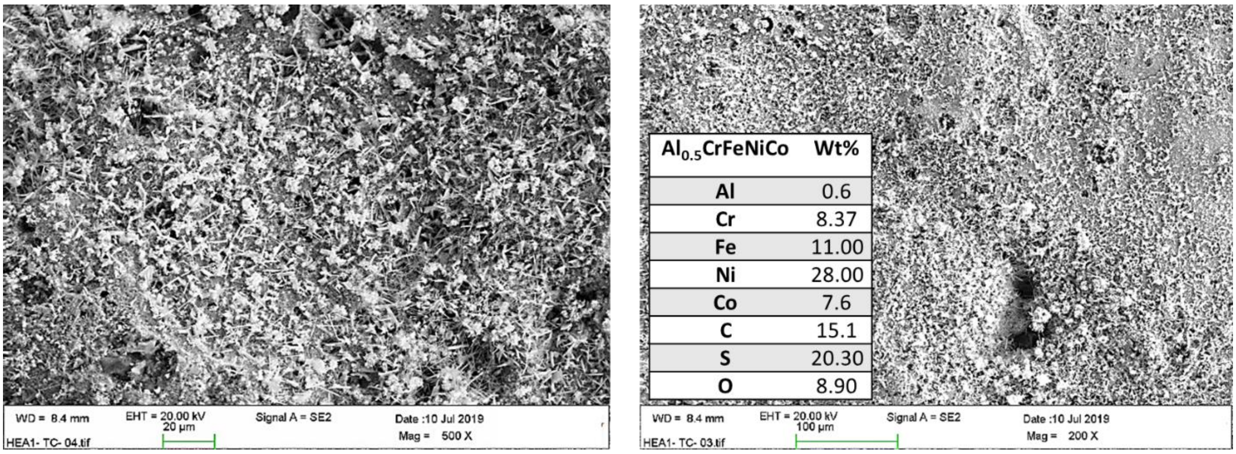

$Al_{0.5}$CrFeNiCo	Wt%
Al	0.6
Cr	8.37
Fe	11.00
Ni	28.00
Co	7.6
C	15.1
S	20.30
O	8.90

(a) (b)

Figure 10: SEM microstructure of $Al_{0.5}$CrFeNiCo coating tested in the simulated geothermal solution with a pH of 4 at T=185 C and P=7 bar: (a) – lower magnification; (b) – higher magnification.

The high temperature here is to be considered as an amplifier of higher rate constants of the solution, leading to the possibility that nickel (Ni) and iron (Fe) actively reacted with sulfur (S), which were found on the $Al_{0.5}$CrFeNiCo surface that can result in forming a passive layer (see the table of Figure 10b). Figure 10b shows corrosion product deposition in the form of "hair/straw" found on $Al_{0.5}$CrFeNiCo surface. Considering the fact that the EDS mapping of the tested $Al_{0.5}$CrFeNiCo coating reveals the more uniform distribution of the elements, where nickel (Ni), iron (Fe), and sulfur (S) found in a higher amount of 28 wt%, 11 wt%, and 20.3 wt%, respectively (see the table of Figure 10b). Therefore, it can be assumed that the formed layer is a corrosion product of nickel sulfide (NiS) and iron sulfide (FeS), which contributed to the passivation of the coating surface. However, the NiS and FeS films are expected to be temporal due to the porosity of the layer, and hence, the corrosion process will be renewed on the surface of $Al_{0.5}$CrFeNiCo coating. Aluminum was detected in the lowest amount of 0.6 wt%, which led to low contribution in the passivation process. It is noted that in both HEA surfaces of CoCrFeNiMo and $Al_{0.5}$CrFeNiCo, the inclusion of sulfur (S) is a result of its deposition from the geothermal solution when reacting to the coating material.

EDS mapping (Figure 11) for the cross-sectioned $Al_{0.5}$CrFeNiCo sample tested under given simulated geothermal conditions has shown the sulfur precipitated in a localized defect of the coating. However, further sulfide penetration down to the substrate was not observed. The tested bulk coating of $Al_{0.5}$CrFeNiCo has contained cracks, and porous layers consisted of complex oxide layers of Cr_2O_3. This indicates that the inner complex oxide layer may be formed due to the redox reaction of Cr and O, which occurred in the regions of longitudinal cracks in the coating.

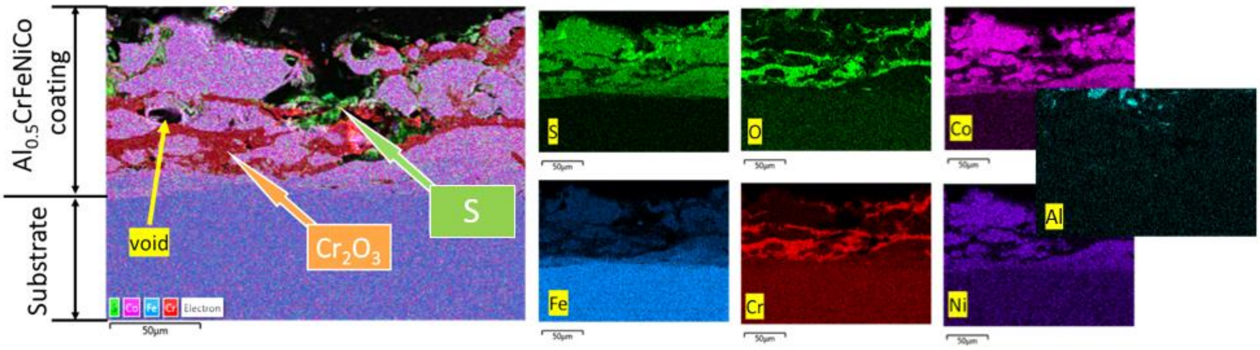

Figure 11: EDS mapping of Al0.5CrFeNiCo coating tested in the simulated geothermal solution with a pH of 4 at T=185 C and P=7 bar.

5. CONCLUSIONS

In this work, we presented the developed laboratory facility for conducting corrosion tests for novel coatings for geothermal applications. The lab facility was developed based on the flow-through process simulating the real geothermal environment. For this purpose, the flow-through reactor was designed with the ability to place metallic samples for corrosion investigation. For the trial corrosion tests, the high entropy alloy coatings of CoCrFeNiMo and $Al_{0.5}$CrFeNiCo were developed. After the corrosion test in the simulated geothermal solution with a pH of 4 at T=185 ºC and P=7 bar over 96 hours, the deposition of a corrosive element such as sulfur was found in both the selected coatings. In the surface of CoCrFeNiMo, the formation of pits was detected being the hotbed of pitting corrosion, whereas $Al_{0.5}$CrFeNiCo coating showed the greater resistance to the nucleation of localized corrosion that can be explained by the nickel and iron inclusions that were involved in the electrochemical reaction with deposited sulfur, that led to spontaneous passivation of the surface coating. It is to be noted here that the formed passive layer is partially protective that temporarily inhibits further corrosion reaction, and consequently, the corrosion process in the coating will be renewed. The cracks and voids were found in the cross-sections of both tested coatings.

5. ACKNOWLEDGEMENT

This work is part of the H2020 EU project Geo-Coat: “Development of novel and cost-effective corrosion resistant coatings for high temperature geothermal applications” funded by H2020 EU project no. 764086. The authors would also like to acknowledge the resources and collaborative efforts provided by the consortium of the Geo-Coat project.

REFERENCES

Stefánsson, A.: Gas chemistry of Icelandic thermal fluids, *J. Volcanol. Geotherm.* Res. 346 (2017) 81–94. doi:10.1016/j.jvolgeores.2017.04.002.

Sigurðardóttir, S. S., Stefánsdóttir, A., Gíslason, P. M., Sigfússon, B., Haraldsdóttir, H., Fanicchia, F.: Report on characterisation of geothermal fluid, *Orka Náttúrunnar*, 2018 (project deliverable D1.3).

Karlsdóttir, S.N.: Corrosion, Scaling and Material Selection in Geothermal Power Production, in: *Compr. Renew. Energy*, (2012). doi:10.1016/b978-0-08-087872-0.00706-x.

Kovalov, D., Ghanbari, E., Mao, F., Kursten, B., Macdonald, D.D.: Investigation of artificial pit growth in carbon steel in highly alkaline solutions containing 0.5 M NaCl under oxic and anoxic conditions, *Electrochimica Acta.* 320 (2019). doi:10.1016/j.electacta.2019.07.065

Kovalov, D., Balazs, F., Engelhardt, G.R., Macdonald, D.D.: Prediction of corrosion fatigue crack growth rate in alloys. Part II: effect of electrochemical potential, NaCl concentration, and temperature on crack propagation in AA2024-T351. *Corrosion Science*. 152 (2019) 130–139. doi:10.1016/j.corsci.2019.03.005

Karlsdottir, S.N., and Jonsson, T.: Hydrogen Damage of Carbon Steel Fragments From the IDDP-1 Geothermal Well, in: *NACE Int.*, (2018).

Karlsdottir, S.N., Geambazu, L.E., Csaki, I., Thorhallsson, A.I., Stefanoiu, R., Magnus, F., Cotrut, C.: Phase Evolution and Microstructure Analysis of CoCrFeNiMo High-Entropy Alloy for Electro-Spark-Deposited Coatings for Geothermal Environment. *Coatings*, 2019, 9(6), 406. https://doi.org/10.3390/coatings9060406

Parkhurst, D. L. and Appelo C. A. J.: Description of input and examples for PHREEQC version 3: a computer program for speciation, batch-reaction, one-dimensional transport, and inverse geochemical calculations, (No. 6-A43) *US Geological Survey*, (2013).

World Health Organization (WHO): Concise International Chemical Assessment Document 53, Hydrogen sulfide: Human health aspects, *WHO:* Geneva, Switzerland, 2003.